



Monitoring Hurricanes Over the Ocean with Wide Swath SAR

Karen S. Friedman and Xiaofeng Li

One of the most unexpected new applications for wide swath synthetic aperture radar (SAR) is the monitoring of atmospheric expressions of storms over the ocean. SAR has an advantage over many sensors because it can pass through clouds and take images at any time of day. However, since SAR's detection capability is based on the modulation of the sea surface wind field, it can only observe storms over water. Hurricanes and other mesoscale storms are easily detected with existing observations, but SAR can contribute fine-resolution low-level information that cannot be seen below the cloud deck with other sensors. Using Radarsat-1, we have imaged three hurricanes during the 1998 season. Two SAR images of Hurricane Bonnie separated by 1 day are presented, and observations from the SAR data are discussed. (Keywords: Atmospheric expressions, Hurricanes, Storms, Synthetic aperture radar.)

INTRODUCTION

Synthetic aperture radar (SAR) data have been used operationally for purposes such as ice and flood monitoring for many years. Recently, new uses for SAR data have been realized. One of the most unexpected is using SAR to image atmospheric storms on the ocean surface.¹ Using Radarsat-1, we have been able to image many types of storms, including polar lows and hurricanes.² Although other existing sensors such as the Advanced Very High Resolution Radiometer (AVHRR) and the Geostationary Orbiting Environmental Satellite (GOES) imager can easily detect hurricanes and other mesoscale storms, SAR can contribute fine-resolution ocean surface information that cannot otherwise be obtained below the cloud deck.

At the National Oceanic and Atmospheric Administration (NOAA) National Environmental Satellite Data Information Service (NESDIS) we actively monitor the Atlantic Ocean off the southeast coast of the United States during hurricane season. Since data acquisitions by Radarsat-1 must be scheduled days in advance, we randomly schedule wide-area coverage of a region rather than wait until a storm appears. This approach has worked well and has resulted in the capture of three hurricane images during the 1998 hurricane season, two of Hurricane Bonnie and one of Danielle, including the latter's entire eye. Efforts by Chris Elvidge of NOAA and Radarsat International resulted in the acquisition of images from two

subsequent hurricanes, Georges and Mitch, also during this period (see Katsaros et al., this issue).

To gain an understanding of storm progression, a time series of SAR images is essential, but it is difficult to obtain more than one image of any particular storm. We did, however, manage to image Hurricane Bonnie twice over the course of 2 days. Although the entire storm does not fit in one ScanSAR wide mode image, it is still possible to sense the evolution of parts of this storm. This article presents SAR imagery of Hurricane Bonnie on 25 and 27 August 1998 and the effectiveness of imaging the hurricanes with Radarsat-1 SAR ScanSAR wide mode data.

DATA SETS AND BACKGROUND

The Canadian Radarsat-1 was launched in November 1995 into a Sun-synchronous polar orbit with an ascending equator crossing time (local time) of 6:00 p.m. It has a 5.6-cm C-band SAR with horizontal–horizontal (HH) polarization and is right-looking. The sensor mode used in this study is ScanSAR wide B, which has a swath width of 500 km. The resolution of the data is 100 m, with a pixel spacing of 50 m.

SAR has an advantage over many sensors because its active radar signal passes through clouds and can image at any time of day. However, since the SAR detects variations in sea surface roughness caused by wind variations, SAR instruments can observe storms only over the water. This is accomplished by detecting the modulation of the sea surface Bragg waves caused by the variation in the wind field due to the storm. Higher wind speeds increase the backscatter, and the wind direction can be inferred by wind rows that have a sea surface roughness signature.^{3,4} Atmospheric attenuation by rain may also result in observed regions of low backscatter.⁵

We used infrared data from channel 4 (11 μm) of GOES-10 to compare atmospheric signatures in the Radarsat-1 SAR data. GOES-10 data were chosen because they are available every 30 min as opposed to data from polar orbiting instruments such as AVHRR. GOES-10, which is operated by NOAA, is a multichannel instrument that senses emitted radiant infrared energy and reflected solar energy from the Earth's surface and atmosphere. The spatial resolution of channel 4 is nominally 4 km at the equator; however, the resolution of a geostationary satellite like GOES-10 decreases significantly above 50°N latitude. A polar orbiter such as Radarsat-1 does not have a latitude-dependent resolution and so has an advantage over geostationary satellites in regions like the Bering Sea.

NEXRAD reflectivity images from the National Climatic Data Center were used to sense the precipitation from Hurricane Bonnie and to confirm that variability in the SAR was correlated with precipitation

variability. It appears possible to image rain-producing cells with SAR. Rain may dampen the capillary waves on the ocean surface, which results in a smoother surface and a region of low backscatter (dark) on the SAR image. This is true for L-band SAR, but not so pronounced for C-band SAR.⁵ A side-view schematic of a thunderstorm cell from a squall line is presented in Fig. 1a, showing the gust front spreading radially ahead of the rain shaft. This structure was seen by Atlas⁶ in a SAR image from the European Remote Sensing Satellite 1 (ERS-1). Atlas believes that the echo-free hole in a SAR image of a storm cell results from a damping of the capillary waves due to the impact of precipitation on the sea surface. Figure 1b is the top view of Fig. 1a, showing the mechanics involved in forming the round-shaped storm cells observed in SAR imagery. The rain dampens the capillary waves and decreases the backscatter intensity. However, low

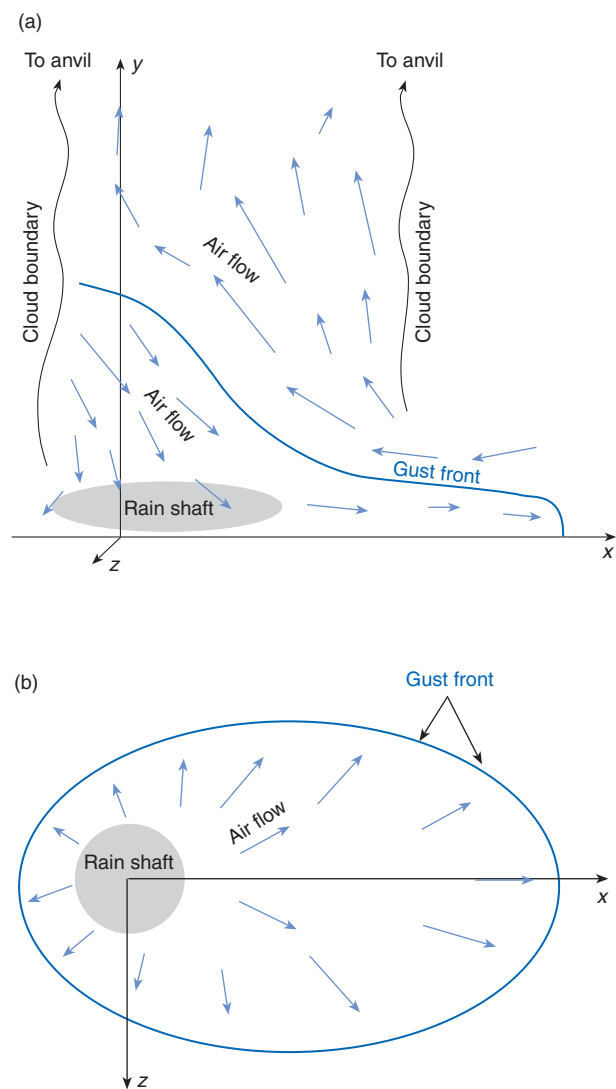


Figure 1. Dynamics of the same squall line viewed from the side (a) and from above (b).

backscatter intensity is not always associated with these round features in a SAR image.

Rain occurs for only 15 to 30 min of the approximate 1-h lifetime of a thunderstorm cell. Rogers and Yau⁷ explain the three stages of a thunderstorm: a cumulus stage, where the updraft through most of the cell lasts for 10 to 15 min; a mature stage, where downdrafts and updrafts accompany rain and last for 15 to 30 min; and a dissipating stage, where there are weak downdrafts through most of the cell. Therefore, storm cells viewed by SAR in the last stage would include imprints from the downdrafts only. Figure 2 shows a storm cell from Radarsat-1 taken in the Bering Sea. The edge of the downdraft can be seen as the rounded formation in the center. The cell is darker on the near-range side of the image, possibly due to differences in wind direction across the cell. As the wind originates from the center and spreads outward, the easterly component cancels out with the ambient wind and causes a region of low wind, and therefore lower backscatter in the SAR image.

HURRICANE BONNIE

On 26 August 1998, at 00 Greenwich Mean Time (GMT), the National Weather Service in Miami, Florida, issued an advisory on Hurricane Bonnie stating that it was moving N-NW at 7.2 m/s (16 mph), with maximum sustained winds of 51.4 m/s (115 mph) and



Figure 2. Radarsat-1 ScanSAR wide B image of a round storm cell (© Canadian Space Agency [CSA], 1998).

minimum central pressure of 95.8 kPa, or 958 millibar (mb). Only 42 min earlier, Radarsat-1 collected data covering the area to the left of the hurricane's eye. Winds in the region covered by the SAR image ranged from 13 m/s near the coast to 18 m/s farther east (taken from an Atlantic Oceanographic and Meteorological Laboratory wind analysis at 0130 GMT on 26 August 1998). Figure 3a superposes the SAR image over a GOES channel 4 water vapor image taken 3 min earlier. This SAR image clearly shows the Gulf Stream

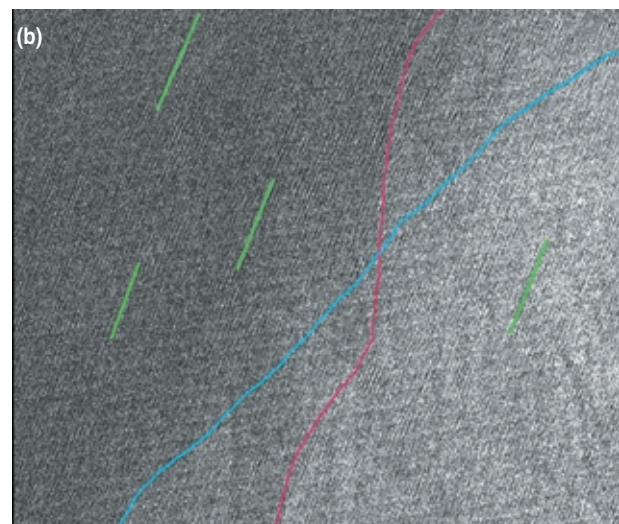
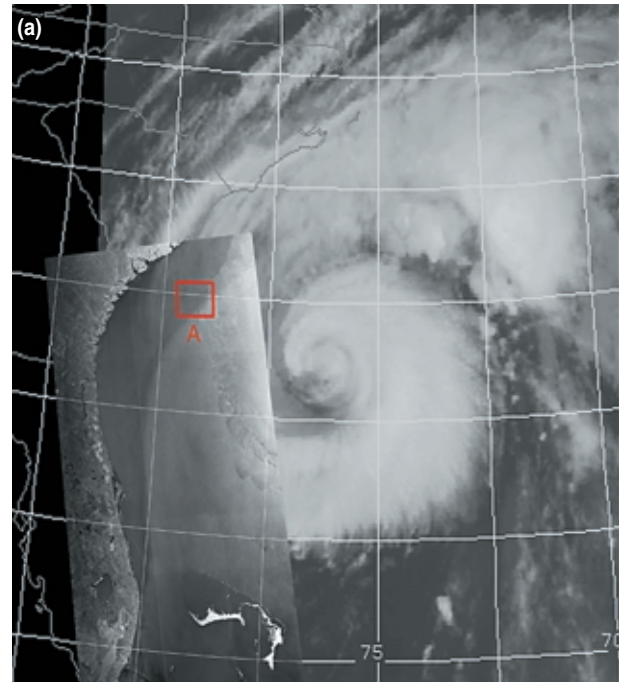


Figure 3. Radarsat-1 ScanSAR wide B image (a) of Hurricane Bonnie on 25 August 1998 at 2318 GMT. SAR image is overlaid on a GOES channel 4 image taken at 2315 GMT. Expanded view (b) is a magnification of box A. The boundary of a downdraft cell is shown in red, the Gulf Stream boundary is shown in blue, and the oceanic long waves are highlighted in green (© CSA, 1986).

coming up from the tip of Florida and crossing the storm cells. These cells, which are visible in the SAR bands, match exactly with the inner side of the large arm spiraling from the hurricane's eye in the GOES image. From the GOES imagery alone, there is no indication of which clouds have associated downdrafts allowing the possible formation of precipitation. But with SAR, downdraft cells are clearly visible. To corroborate our claim that these are indeed bands of convective storms capable of forming rain, we looked at the NEXRAD imagery (Fig. 4a) at 23 GMT, which shows rain in the same region as the storm cells in the SAR.

The Gulf Stream is known to be visible by radar.^{8,9} Its warm water can produce an unstable marine atmospheric boundary layer that leads to increased surface drag and increased Bragg spectral energy density, therefore increasing the radar backscatter.⁹ Figure 3b, an

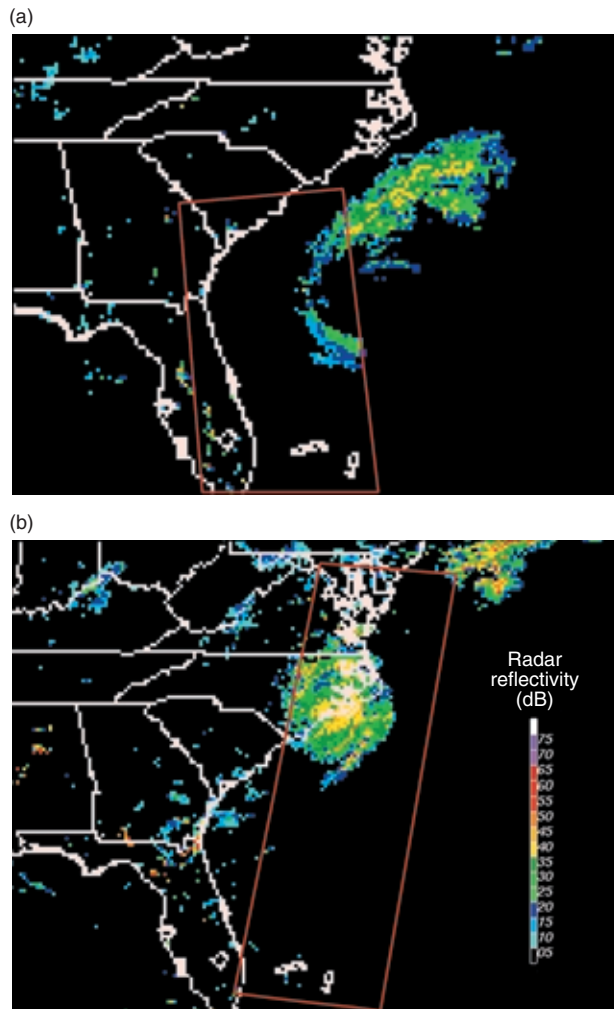


Figure 4. A NEXRAD reflectivity image for (a) 25 August 1998 at about 23 GMT and (b) 27 August 1998 at about 11 GMT. Red boxes indicate approximate locations of SAR image in Figs. 3 and 5, respectively.

expanded view of the box marked “A” in Fig. 3a, shows the intersection of the Gulf Stream boundary (in blue) with the downdraft cell boundary (in red). The Gulf Stream region has a higher backscatter (lighter in color), as would be expected. Its location would normally be extremely difficult to detect using other types of satellite data when the region is covered so completely by clouds as it is during a hurricane. SAR is important as a Gulf Stream locator tool when other sensors are unable to view the ocean surface beneath the hurricane clouds. This difference in backscatter intensity between the Gulf Stream region and the region above it *does* lessen after crossing the storm front, but it is still clearly visible. Oceanic long waves caused by the hurricane-produced ocean swell are seen across this entire subset image. A few of these waves are highlighted in green in Fig. 3b. The wavelength as measured from the SAR image is approximately 350 m. The waves are aligned parallel to the hurricane band and change direction slightly when crossing the Gulf Stream front or the storm front.

A second image of Hurricane Bonnie taken by Radarsat-1 on 27 August 1998 at 1108 GMT is shown in Fig. 5a over a coincident GOES image. The eye of the storm has just made landfall in North Carolina. The National Weather Service advisories closest in time to the SAR pass were 9 and 13 GMT. They list the maximum sustained winds at 38 m/s (85 mph) and 33.5 m/s (75 mph), respectively. These winds were much weaker than when the hurricane was previously imaged. The minimum central pressure was listed at 97 kPa (970 mb) and 97.5 kPa (975 mb), respectively, which further indicated a weakening of the storm. There is a thin line of convective cells with rain indicated by darker areas with low backscatter intensity. This matches up with an arm of rain seen in the NEXRAD image at 11 GMT (Fig. 4b). These dark areas, within the red box marked “B” in Fig. 5a, are seen at higher resolution in Fig. 5b overlaid with the NEXRAD imagery. The NEXRAD image shows areas associated with moderate-to-heavy precipitation that correspond to the dark regions of low backscatter on the SAR. This finding would indicate that these regions of low backscatter are formed by precipitation. They are not associated with the round convection cells seen in the SAR imagery on 27 August, possibly due to different wind and atmospheric conditions.

Oceanic swell is not seen in this image as was seen on 25 August, but internal waves are observed in Fig. 5a in the region marked “C”. These are believed to be internal waves because their wavelength is approximately 1.3 km, which is conceivable for internal waves and much longer than oceanic swell. Internal waves on SAR of tidal origin have been noted frequently^{10–12} (see also the article by Li et al. elsewhere in this issue). The internal waves in the 27 August case, however,

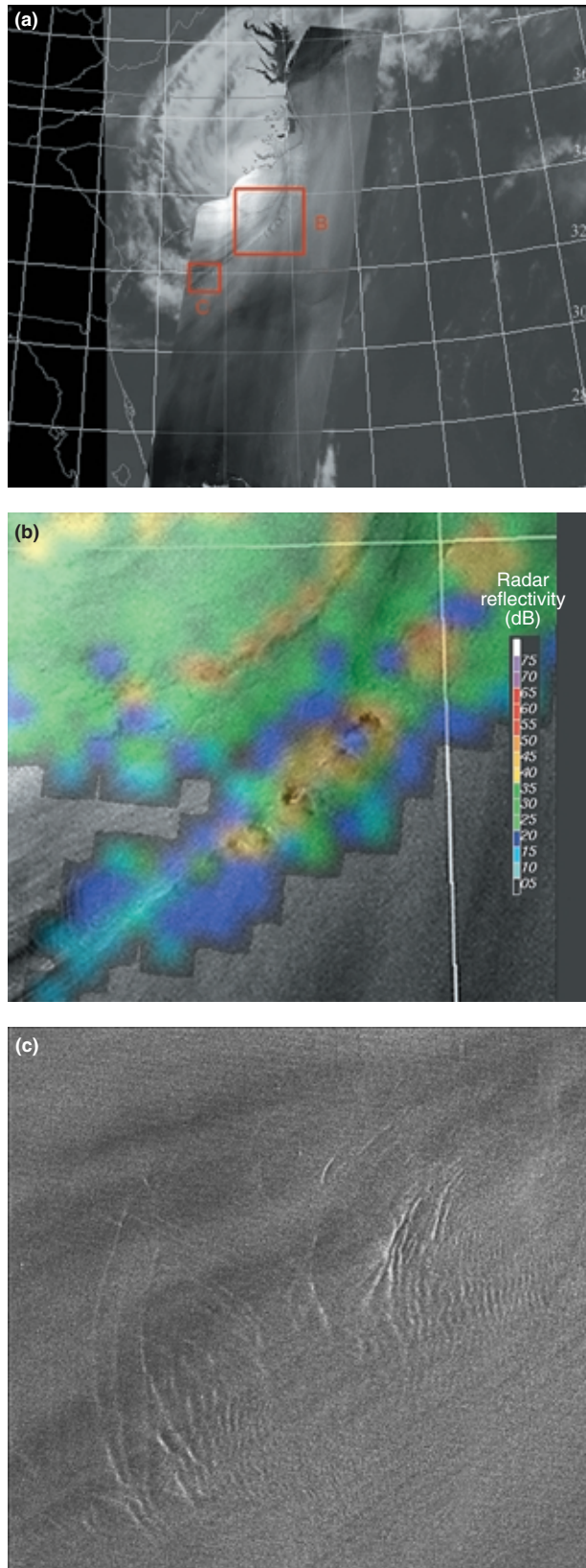


Figure 5. Radarsat-1 ScanSAR wide B image (a) of Hurricane Bonnie (27 Aug 1998) at 1108 GMT. SAR image is overlaid on the GOES channel 4 image taken at 1115 GMT. Boxes B and C are shown at higher resolution in (b) and (c), respectively. A NEXRAD reflectivity image at the same time is placed over the SAR image in Fig. 4b (© CSA, 1998).

may be caused by wind forcing of the thermocline, although we cannot say that there is not another source. By looking more closely at region “C” in Fig. 5c, we can see that these waves are traveling mainly in a southwesterly direction along the wind rows emanating along the same arm of the hurricane that produced the rain in region “B” (Fig. 5b). The wind rows can be seen in Fig. 5c as alternate lighter and darker stripes of varying thickness.

SUMMARY

With a continuous SAR data acquisition campaign, it is possible to catch a slow-moving storm with a long lifetime more than once. In this article we have presented Radarsat-1 imagery of Hurricane Bonnie off the Atlantic Coast in 1998 on two separate occasions. The scale of this storm is larger than the 500-km swath width of Radarsat-1 ScanSAR wide mode, thus making it impossible to image the entire storm at once. The best-case scenario would have been to have a SAR image on each day, with the hurricane centered within each pass, and to have both of these passes occur when the hurricane was completely over water.

This pair of Hurricane Bonnie SAR images includes signatures of convective storms, although the signatures differ on each day. The large, round storm cells seen on 25 August are not the same as those seen on 27 August, where regions of low backscatter with no circular downdraft boundaries are seen. The image on 25 August shows the Gulf Stream boundary, even as it crossed convection cells. Oceanic long waves covered large portions of this image and also crossed the downdraft cells and Gulf Stream without interruption. The SAR image on 27 August did not contain oceanic swell, but did have internal waves with wavelengths over 1 km. It is also seen that SAR may have the ability to see small-scale wind and rain events. Our data collection effort for the 1999–2000 seasons will build on our progress to date.

REFERENCES

- Johannessen, J. A., Shuchman, R. A., Johannessen, O. M., Davidson, K. L., and Lyzenga, D. R., “Synthetic Aperture Radar Imaging of Upper Ocean Circulation Features and Wind Fronts,” *J. Geophys. Res.* **96**, 10,411–10,422 (1991).
- Friedman, K., Pichel, W. G., and Li, X., “Mesoscale Oceanic and Atmospheric Feature Detection Through Fusion of RADARSAT SAR with GOES/Imager Data,” in *Proc. IEEE Int. Geoscience and Remote Sensing Symp.*, pp. 907–909 (1998).
- Monaldo, F. M., and Beal, R. C., “Toward Real-Time Processing, Blending, and Dissemination of Operational Wind Products from the RADARSAT SAR,” in *Proc. IEEE Int. Geoscience and Remote Sensing Symp.*, pp. 959–961 (1998).
- Beal, R. C., and Pichel, W. G., “Stormwatch 97–98 and Beyond: Application of SAR as a High Resolution Scatterometer in Coastal Regions,” in *Proc. IEEE Int. Geoscience and Remote Sensing Symp.*, pp. 1379–1381 (1998).
- Alpers, W., Gade, M., Melsheimer, C., Bao, M., Masuko, L., and Kobayashi, T., “The Imaging of Different Oceanic and Atmospheric Phenomena by SIR-C/X-SAR,” in *Proc. IEEE Int. Geoscience and Remote Sensing Symp.* (1995).

- ⁶Altas, D., "Origin of Storm Footprints on the Sea Seen by Synthetic Aperture Radar," *Science* **266**, 1364–1366 (25 Nov 1994).
- ⁷Rogers, R. R., and Yau, M. K., "A Short Course in Cloud Physics," in *International Series in Natural Philosophy*, D. Ter Haar (ed.), Pergamon Press, New York (1976).
- ⁸Weissman, D. E., Thompson, T. W., and Legeckis, R., "Modulation of Sea Surface Radar Cross Section by Surface Stress: Wind Speed and Temperature Effects Across the Gulf Stream," *J. Geophys. Res.* **85**(C9), 5032–5042 (20 Sep 1980).
- ⁹Beal, R. C., Kundryavtsev, V. N., Thompson, D. R., Grodsky, S. A., Tilley, D. G., et al., "The Influence of the Marine Atmospheric Boundary Layer on ERS 1 Synthetic Aperture Radar Imagery of the Gulf Stream," *J. Geophys. Res.* **102**(C3), 5799–5814 (15 Mar 1997).
- ¹⁰Fu, L.-L., and Holt, B., "Seasat Views Oceans and Sea Ice with Synthetic-Aperture Radar," JPL Publ. 81–120, Pasadena, CA (1982).
- ¹¹Apel, J. R., and Gonzalez, F. I., "Nonlinear Features of Internal Waves off Baja California as Observed from the SEASAT Imaging Radar," *J. Geophys. Res.* **88**(C7), 4459–4466 (20 May 1983).
- ¹²Porter, D. J., and Thompson, D. R., "Continental Shelf Parameters Inferred from SAR Internal Wave Observations," *J. Atmos. Oceanic Technol.* **16**, 475–487 (1999).

ACKNOWLEDGMENTS: Thanks to William G. Pichel and Pablo Clemente-Colón for their contributions to this article. This research was funded by the NOAA/NESDIS Ocean Remote Sensing Program as part of the NESDIS Monitoring and Detection (NEMoDe) project. RADARSAT data were obtained under NASA RADARSAT ADRO Project #396 and processed at the Alaska SAR Facility.

THE AUTHORS

KAREN S. FRIEDMAN is with NOAA/NESDIS in Camp Springs, MD. Her e-mail address is kfriedman@nesdis.noaa.gov.

XIAOFENG LI is with NOAA/NESDIS in Camp Springs, MD. His e-mail address is xiaofeng.li@noaa.gov.